AIAA Aviation
22-26 June 2015, Dallas, TX
21st AIAA/CEAS Aeroacoustics Conference

Acoustical Environment of an F-35B Aircraft During Vertical Landings

Brent Reichman[1]
Brigham Young University, Provo, UT, 84602

J. Micah Downing[2]
Blue Ridge Research and Consulting, LLC, Asheville, NC, 28801

Allan Aubert[3]
US Navy, Naval Air Systems Command, Patuxent River, MD, 20670

Richard L. McKinley[4]
Air Force Research Laboratory, Wright-Patterson Air Force Base, OH, 45433

Kent L. Gee[5] and Tracianne B. Neilsen[6]
Brigham Young University, Provo, UT, 84602

Alan T. Wall[7]
Air Force Research Laboratory, Wright-Patterson Air Force Base, OH, 45433

And

Michael M. James[8]
Blue Ridge Research and Consulting, LLC, Asheville, NC, 28801

Measurements of the sound field near an F-35B during vertical landing operations are reported. Data are presented and discussed from the approach, hover, and descent of the aircraft, and compared with ground run-up measurements. Overall levels are comparable to published values for the F-35A at 50% engine thrust ratio during ground run-ups. One-third-octave spectra are also presented, and spectra from various stages of the approach and landing are compared. Changes in the spectral shape during the landing process are discussed and impingement is presented as a possible cause of these changes. The azimuthal directivity of the sound field during hover and descent are shown for the purpose of environmental modeling, showing slight directivity during the hover process and little to no directivity during the descent. An analysis of nonlinear propagation metrics gives values again consistent with those found for the F-35A operating at 50% engine thrust ratio during ground run-up.

[1] Ph.D. Candidate, Dept. of Physics and Astronomy, N283 ESC.
[2] Chief Scientist, 29 N Market St, Suite 700, AIAA Member.
[3] Senior Technical Specialist – Noise & Emissions Team Lead, NAVAIR Propulsion & Power, Bldg 106 rm 229c, 22195 Elmer Rd., AIAA Senior Member
[4] F-35 Performance & Specialty Engineering Acoustics Lead, Battlespace Acoustics Branch, 2610 Seventh St., Bldg. 441, Wright-Patterson AFB, OH 45433.
[5] Associate Professor, Dept. of Physics and Astronomy, N283 ESC, AIAA Senior Member.
[6] Part-Time Assistant Professor, Dept. of Physics and Astronomy, N283 ESC, AIAA Member.
[7] Postdoctoral Fellow, Battlespace Acoustics Branch, 2610 Seventh St., Bldg. 441, Wright-Patterson AFB, OH 45433, AIAA Member.
[8] Senior Principal Engineer, 29 N Market St, Suite 700, AIAA Member.

Nomenclature

ASF	=	average steepening factor
dSk	=	derivative skewness
ETR	=	engine thrust request
L_{eq}	=	equivalent level, dB re 20 μPa
OASPL	=	overall sound pressure level, dB re 20 μPa
OTO	=	one-third octave
σ	=	standard deviation
SPL	=	sound pressure level, dB re 20 μPa
STOVL	=	short take off and vertical landing
VL	=	vertical landing

I. Introduction

THE acoustical environments of fifth-generation military jet aircraft (F/A-18E, F-22A, and F-35) have been more significantly documented in the scientific literature than prior aircraft.[1-5] However, the short take-off and vertical landing (STOVL) capability of the F-35B represents a more complicated environment than for traditional aircraft. Though both the A and B variants of the F-35 are driven by a Pratt and Whitney F135 engine,[6] the F-35B is equipped with the Rolls-Royce LiftSystem®,[7] consisting of the Rolls-Royce LiftFan®, Driveshaft, a three-bearing swivel module (3BSM), and two Roll Posts, one located on each wing. During vertical landing (VL), the LiftFan is driven by turbines in the engine, capable of providing 20,000 lbf cold thrust. The Roll Posts can provide an additional 1,950 lbf thrust each. The 3BSM rotates downwards, providing an additional 18,000 lbf dry thrust, which corresponds to roughly 65% ETR.[6] The two lower-power sound sources may fundamentally alter the noise field from the operating conditions for normal flight. In addition, at low altitudes the downward-facing jet plume can impinge on the landing surface, further changing the noise source.[8] Discrete-frequency tones have been reported for jets impinging on flat plates as early as 1961,[9] and efforts since have sought to develop and verify physical models[10] and measure the acoustic field generated for impinging jets.[11,12] This paper addresses some of the changes in the sound field as a result of these changes in the source characteristics.

Figure 1. Vertical landing of an F-35B. *An F-35B lands on aboard the USS Wasp during August 2013. In order to perform a vertical landing, the three-bearing swivel module rotates the engine exhaust nozzle to face downward and the LiftFan® operates near the front of the aircraft. Photograph in the public domain.*[13]

This paper examines the acoustical environment around an F-35B during VL. First, the measurement setup is explained. Next, equivalent sound pressure levels (L_{eq}) and one third-octave (OTO) band spectra are shown for specific microphones during the landing process, including approach, hover, and descent. These levels and spectra provide a brief look at the polar directivity of the noise and are inspected for evidence of impingement noise during the aircraft descent. Spatial maps of sound pressure levels are then presented to show the directionality of the noise radiation, showing slightly directivity in the hover condition and little to no directivity during the descent. Finally, waveform analyses are conducted to examine the noise radiation for nonlinear propagation effects, which for areas near the aircraft during the descent are shown to be comparable to effects observed in ground run-up noise at approximately 50% ETR engine power. [14,15]

II. Experiment Layout

The F-35B VL measurements were performed in Yuma, Arizona in September 2013. The data were collected jointly by Navair and the Air Force Reasearch Laboratory (AFRL), with analysis performed by Navair, AFRL, Blue Ridge Research and Consulting, LLC, and Brigham Young University. The VL measurements were conducted between 3:00 and 9:00 AM local time because of operational constraints imposed by ambient temperatures. The terrain was essentially flat and consisted of asphalt outfield areas and concrete runways, both of which provide a very rigid and acoustically reflective surface. Temperatures varied from 24.5°C to 31°C, with an average wind speed of around 2.5 mph.

A total of 45 microphones were used in three semicircular arcs with radii of 76.2, 152.4, and 304.8 m (250, 500, and 1000 ft) from the origin, which was centered on the touchdown pad as shown in Fig. 2. (For convenience, references to the different arcs are made in feet hereafter.) In addition, 12 microphones were suspended from two cranes, one located just outside the 500 ft arc, the other just outside the 1000 ft arc. However, the results from these microphones are not discussed in this paper. In order to simplify orientation, the 0° orientation angle for the array was pointed to the northeast from the touchdown pad, and 180° is exactly opposite to the southwest. The 250 foot arc had seven microphones each spaced 30° apart. The 500 and 1000 foot arcs both had 19 microphones spaced 10° apart. Two microphones in the 1000 ft arc, located at 0 and 10°, needed to be placed closer to the aircraft due to constraints at the landing site, at 700 and 750 ft respectively. The microphones in the 250, 500, and 1000 ft arc were located at heights of 5, 12, and 30 ft above the ground, respectively.

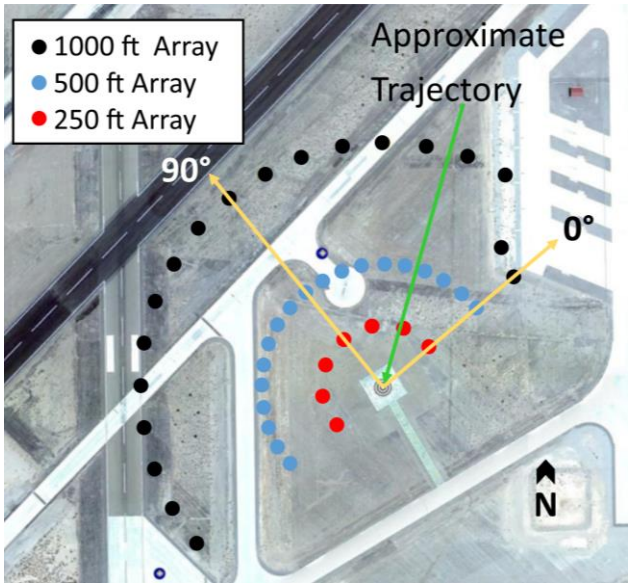

Figure 2. The experiment layout. *Forty-five microphones placed in three arcs, located at 76.2, 152.4, and 304.8 m (250, 500 and 1000 ft). The arcs at 500 and 1000 ft had 19 microphones, spaced 10° apart, and the 250 ft arc consisted of seven microphones spaced every 30°. Due to space constraints, the microphones at 0° and 10° in the 1000 ft arc were moved closer to the source, at distances of approximately 700 and 750 ft. The microphones that will be used extensively in this paper lie along the* 30° *and* 90° *radials, giving information near the path of the aircraft and removed from it.*

The VL process can be divided into several subcategories: approach, hover, descent, and touchdown. During approach, the aircraft maintains a roughly constant elevation while nearing the touchdown site. During hover, the aircraft maintains constant elevation and position directly over the touchdown site, and during descent the aircraft maintains a near constant position over the touchdown pad while elevation decreases. Because the mechanisms behind the hover and descent processes differ so drastically from normal flight they are of the most interest to our current study. The trajectories for the four VL from the September 2014 measurements were similar, as seen in Fig. 3; the aircraft approached roughly from the north-northeast, from approximately 30° angle of the array. Slight

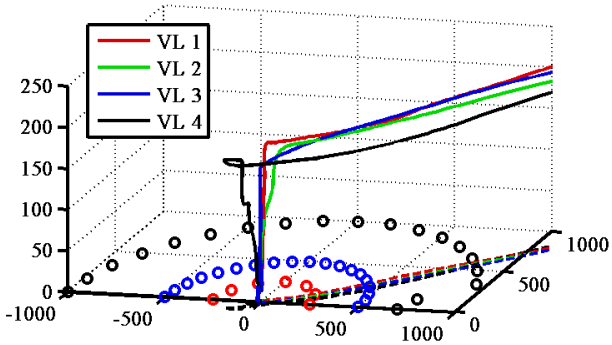

differences in the aircraft trajectory are evident near the hover stage. The data and analyses presented in this paper focus primarily on VL 2.

Figure 3. Vertical Landing Trajectories. *The trajectories of the F-35B during four VLs. The three microphone arcs are illustrated as black (1000 ft), blue (500 ft), and red (250 ft) circles. Data primarily from VL2 is analyzed in this paper.*

III. Results

A series of analyses performed on the F-35B VL data help characterize the temporal and spectral properties of the noise sources. Quarter-second, A-weighted L_{eq} values for specific microphones as a function of time yield the source levels during the approach, hover, and descent. Spatial maps across the measurement aperture show the corresponding changes in directionality of the noise. In addition to overall levels, OTO band spectrograms indicate the variation in spectral content throughout the landing. Finally, a preliminary investigation bounds the strength of nonlinear effects.

A. Equivalent Level Time Histories

The variation in the noise levels during the VL is examined by observing both the flat and A-weighted, 0.25-s L_{eq} for six microphones, two microphones in each arc of the array. The microphones used in Fig. 4 are located approximately underneath the approaching aircraft (at 30° array angle) at distances of (a) 1000 ft, (b) 500 ft, (c) 250 ft, while the microphones in Fig. 5 are located at an array angle of 90° (approximately NNW in Fig. 2) for the same distances. Though the results displayed are for VL2, similar results are seen for each of the other VLs. Dashed black lines differentiate the phases of the vertical landing: the timing of the aircraft passing over the 1000, 500, and 250 ft arcs, and the beginnings of the hover and descent portions.

Trends seen in all of the plots in Figs. 4 and 5 provide physical insight into the resultant noise field. For the three microphones located underneath the aircraft flight track in Fig. 4, peaks in the L_{eq} are seen shortly before and after the aircraft flies over each microphone. The maximum levels observed at the peaks are between 125-130 dB for all three microphones, a level consistent with findings reported by Gee *et al.*[14] for the static ground run-up noise of the F-35 AA-1 at approximately 50% ETR at 38 m (125 ft). In between the two peaks, a large dip in L_{eq}, likely related to the "cone of silence" that occurs near the jet exhaust plume, is seen. During the approach, the engine nozzle is not pointed directly down as the aircraft approaches the landing pad but is directed slightly behind the aircraft, which explains why the drop in level occurs shortly after the aircraft passes over each microphone. Microphones that are farther removed from the flight path do not exhibit as great of temporal variation in level, but they have roughly constant levels during the approach portion of the vertical landing. For example, as shown in Fig. 5, the 0.25-s L_{eq} for the three microphones along the 90° array angle each stays within a range of 5 dB as the aircraft approaches.

As the aircraft begins its descent approximately 25 seconds before touchdown, the L_{eq} values for all microphones experience a greater variability. As shown in Fig. 4(c) and Fig. 5(c), the microphones located along the 250 ft arc decrease by an average of 10 dB for -20 s< t < -10 s, while microphones at 500 ft and 1000 ft along the 30° radial in Fig. 4(a)-(b) have roughly constant level, whereas those along the 90° array angle in Fig. 5(a)-(b) have more variability. The closer microphones experience a greater change because there is a larger change in polar angle relative to the axis of the engine exhaust. Gee *et al.*[14] reported a similar approximate 10 dB change for that range of polar angle.

Finally, as the aircraft gets closer to the ground, approximately 6-8 s before touchdown for all microphones, a small peak can be seen in the L_{eq}. This peak occurs as the aircraft reaches an altitude of approximately 50 ft, pointing to the possibility that this peak is due to the initiation of impingement of the jet plume on the landing surface. As the aircraft continues to descend, the L_{eq} of all microphones in both figures drops rapidly. This rapid change is likely due to the significant modification of the turbulent noise source as the aircraft continues to descend. Another important feature of the descent process is that the levels in Fig. 4 are comparable to those in Fig. 5, indicating very little azimuthal variation in the L_{eq}.

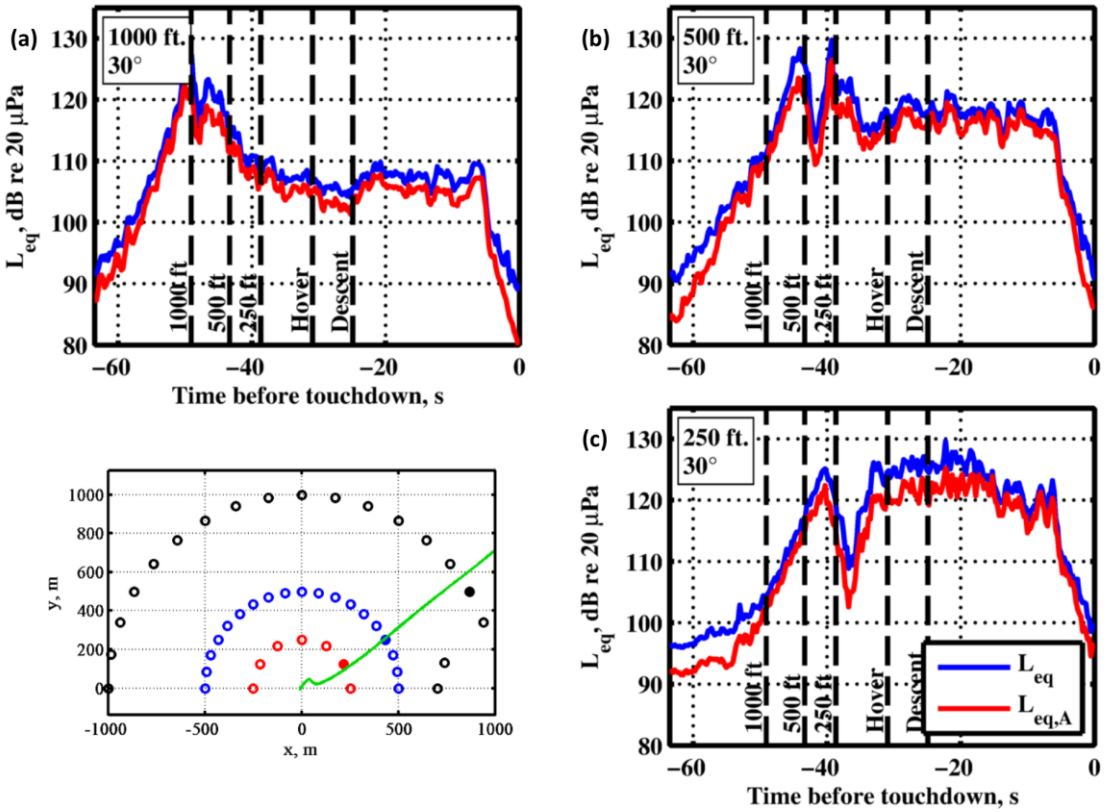

Figure 4. Equivalent levels along the trajectory of the aircraft. *The flat and A-weighted L_{eq} for microphones located near the trajectory of the aircraft (a) at 1000 ft, (b) at 500 ft, and (c) 250 ft from the touchdown pad. The microphones used are shown with respect to the arc and the trajectory of the aircraft as filled-in circles along the 30° radial. The L_{eq} is calculated using 0.25 s sections of the recorded waveform, and the A-weighted levels are calculated after a time-domain filter has been applied to the entire waveform.*

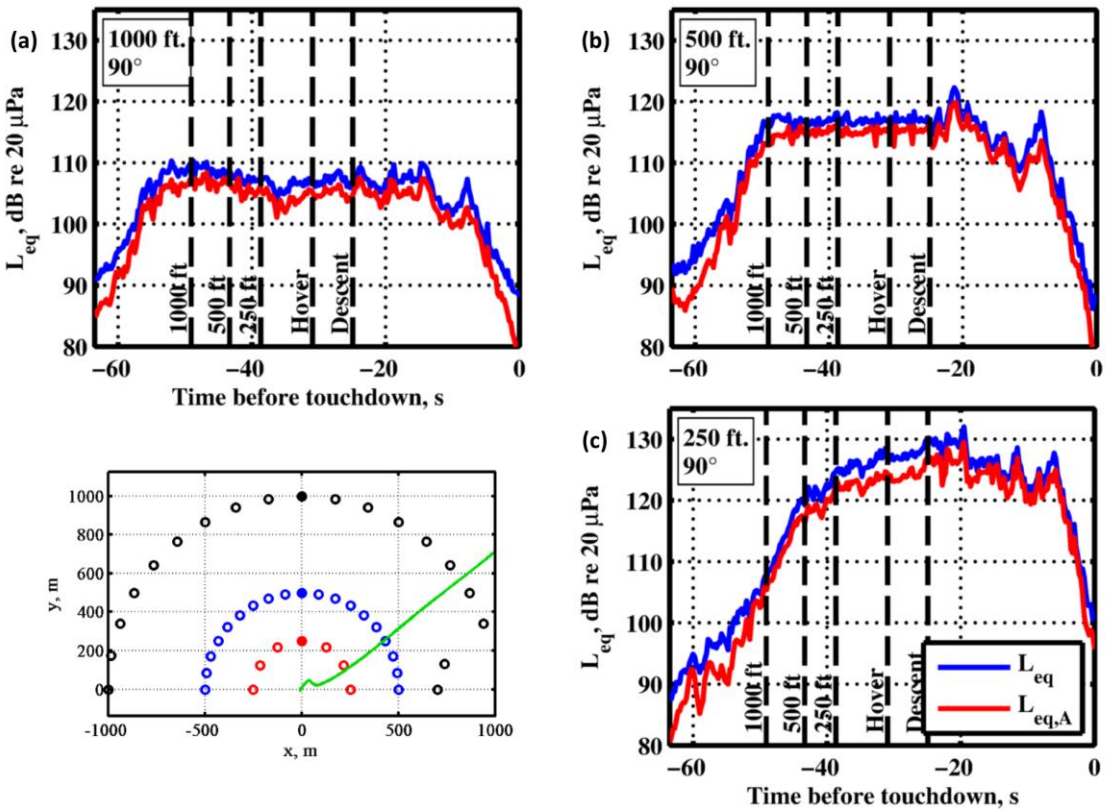

Figure 5. Equivalent levels away from the aircraft. *The flat and A-weighted* L_{eq} *for microphones located at 90° in the local orientation (a) at 1000 ft, (b) at 500 ft, and (c) 250 ft. The microphones used are shown with respect to the arc and the trajectory of the aircraft as filled-in circles along the* 90° *radial. The* L_{eq} *is calculated using 0.25-s sections of the recorded waveform, and the A-weighted levels are calculated after a time-domain filter has been applied to the entire waveform.*

A change in the azimuthal directionality of the noise during the VL process is visible in spatial maps of the L_{eq} for different times during the VL, as plotted in Fig. 6. During the approach, the combination of the aircraft position and the orientation of the engine nozzle results in both polar and azimuthal directionality. Regions of high levels are observed on either side of the exhaust with a region of reduced level in between them. This dip in L_{eq} values is similar to the dip observed after the jet passes over the microphones in Fig. 4. A slight directionality can be seen for the hover condition, but during the landing, the L_{eq} varies less with azimuthal angle.

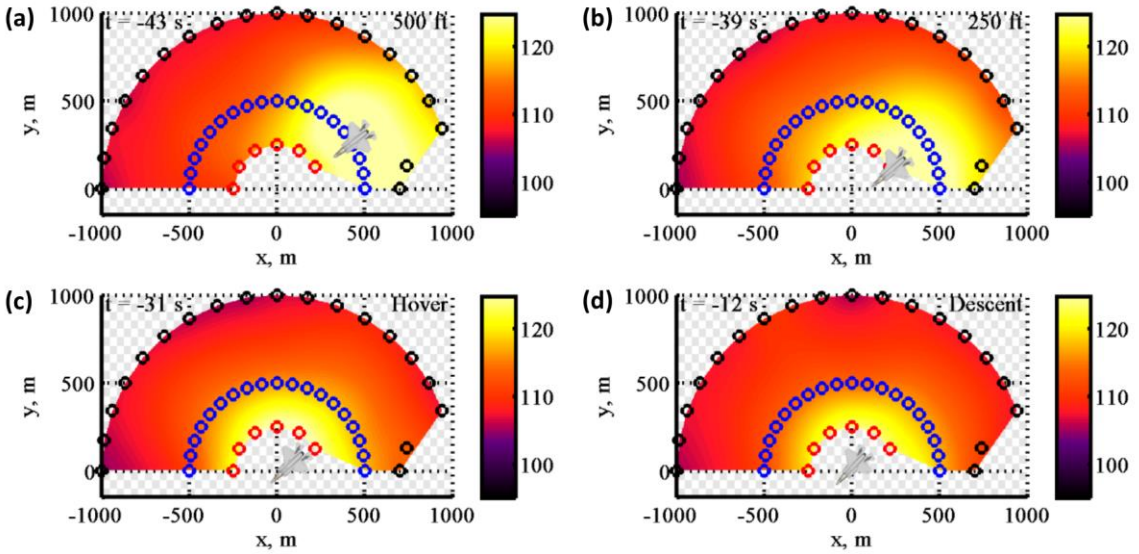

Figure 6. Spatial maps of L_{eq} for multiple aircraft locations. *One-second L_{eq} across the measurement aperture for four events: (a) –(b) as the aircraft passes over the 500, and 250 ft arcs, respectively, (c) as the aircraft is hovering, and (d) as the aircraft descends. The circles indicate the microphone positions. Note: Aircraft not to scale.*

A final comment on the equivalent levels relates to the differences caused by applying the A-weighting. The A-weighted L_{eq} seen in Fig. 4 and Fig. 5 appear to closely mirror the flat-weighted L_{eq}. Fig. 7 shows the difference in the flat and A-weighted levels for the microphone located at 250 ft and 30°, with the difference in L_{eq} caused by A-weighting generally ranging between 2 and 6 dB. An important observation is that the greatest change due to A-weighting is seen shortly before and after the aircraft passes over the microphone. The values with more than a 6 dB ΔL_{eq} correspond to the relative null in seen for -38 s $< t <$ -35 s in Figure 4(c), and values of more than 4 dB ΔL_{eq} are seen corresponding to the two peaks seen at $t =$ -40 and -32 seconds. This trend is also observed for the microphones located at 500 and 1000 ft. Because A-weighting penalizes low-frequency bands, it is likely that the difference in level seen as the aircraft passes over is due to the downward shift of the peak spectral content to low frequencies within the main directivity lobe of the jet around the time the aircraft passes over.

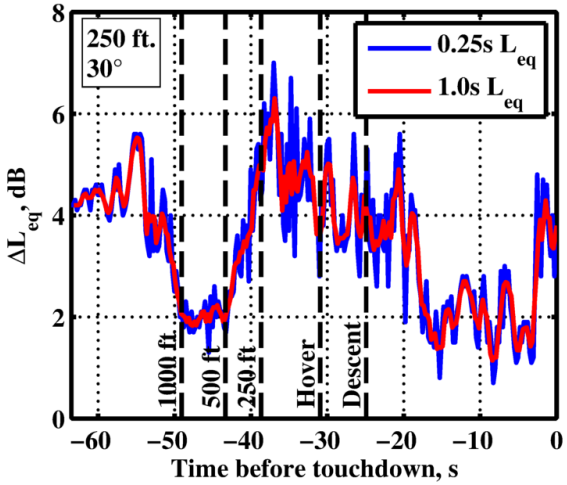

Figure 7. Difference between flat and A-weighted levels. *The decibel change in L_{eq} due to A-weighting as a function of time for the microphone located at 250 ft and 30°. The difference is typically around 3 dB, but can be as large as 7 dB in some cases, such as shortly after the jet flies over the microphone. This trend is evident for all microphones located under the trajectory of the jet.*

B. One-third-octave band spectral time histories

The level-based analyses are complemented by examination of the OTO band spectra. Specifically, the spectra help identify variation in noise content occurring during the stages of the VL process. As before, the spectra are calculated using 0.25-s intervals. Results are shown in Figure 8 and Figure 9 from VL2, for the same microphones examined in Figure 4 and Figure 5 and, again, are representative of all four VLs. During the approach, these spectra have the general characteristics one would expect from jet noise, the spectral shape is rounded when the polar angle between the jet plume and the microphone location is large. When the microphone is in the Mach wave radiation (maximum directivity) region of the jet, the spectral shape is more peaked with a center frequency of a few hundred hertz. As observed in the plots of L_{eq}, a reduction in the spectral levels occurs after the aircraft passes over the microphones along 30°. In addition to the reduction in level after the aircraft passes overhead, interference nulls can be seen for all microphones. These destructive interference nulls are dependent on the microphone position and the aircraft position. The frequency at which the nulls occur are lower when the aircraft is nearly directly above the microphone, and rise as the aircraft is farther away. Another important feature of the spectra is the additional low-frequency noise present during the descent process, approximately 8-10 s before touchdown. This noise diminishes the effect of the interference null and is visible in all three spectra. This noise is possibly due to the impingement of the jet plume on the landing surface.

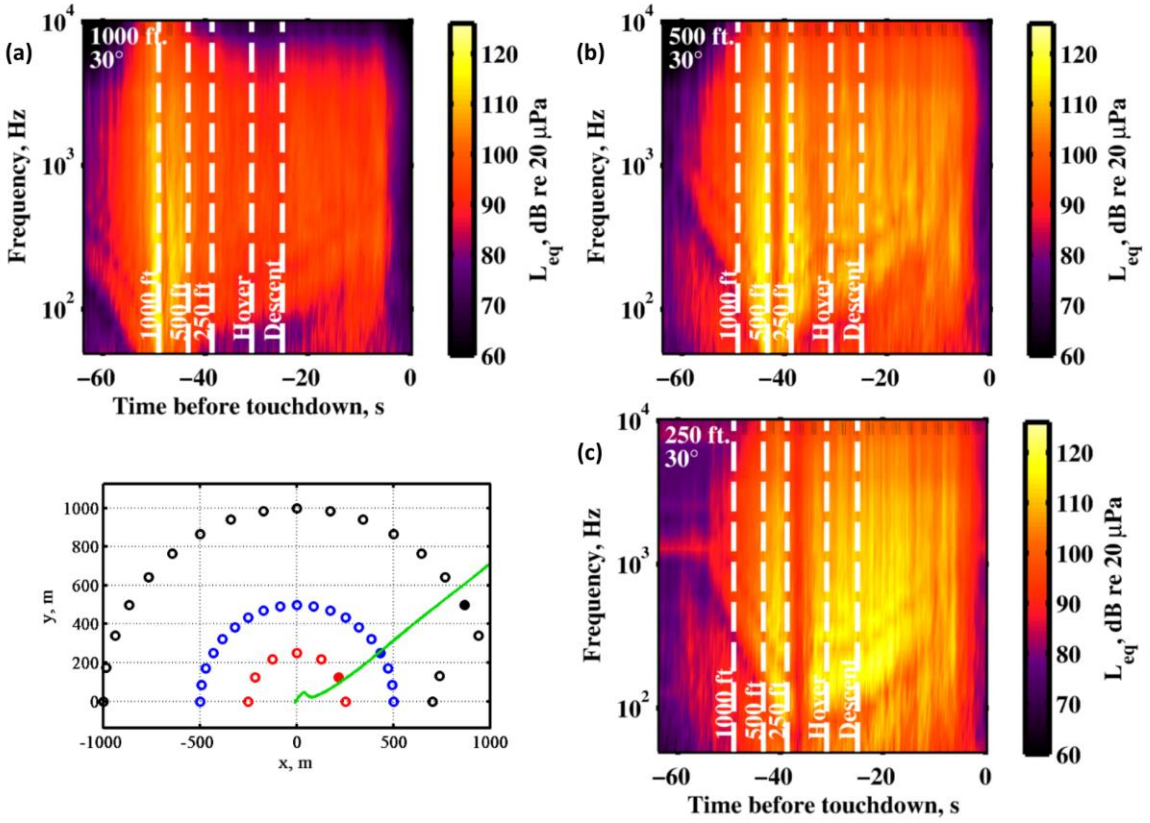

Figure 8. Spectrogram observed along the trajectory of the aircraft. *Time-varying OTO spectra for the same microphones that were used in Figure 4, approximately underneath the trajectory, (a) at 1000 ft, (b) at 500 ft, and (c) 250 ft. The microphones used are shown with respect to the arc and the trajectory of the aircraft as filled circles along the* 30° *radial. Spectra are calculated using quarter-second sections of the waveform. Interference nulls change frequency as the location of the aircraft changes due to the difference in path length between the direct and reflected sound fields.*

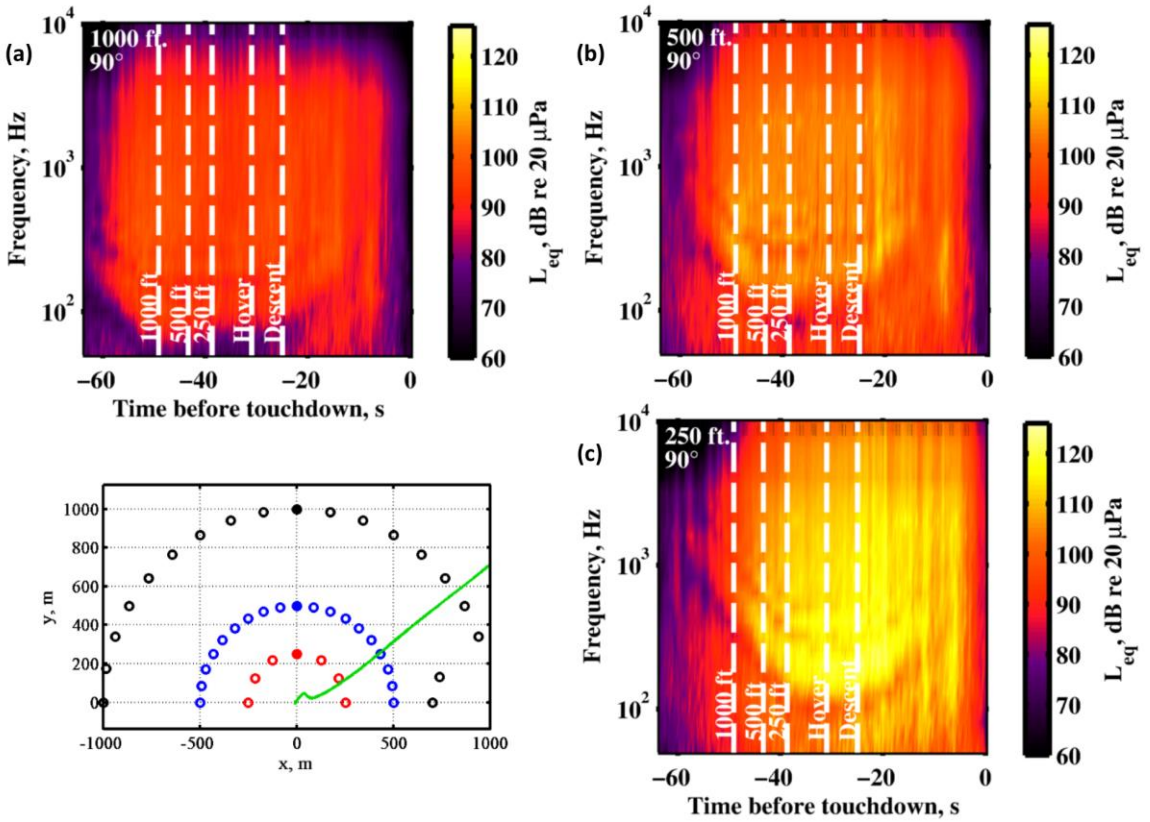

Figure 9. Spectra observed away from the aircraft. *Time-varying OTO spectra for the same microphones as Figure 5, at* 90°*, calculated using quarter-second sections of the waveform. The microphones used are shown with respect to the arc and the trajectory of the aircraft as filled-in circles along the* 90° *radial. As in Figure 8 interference nulls can be seen due to the difference in path length from the direct and reflected sound, As the plane descends these nulls are washed out due to noise produced as the plume impinges on the landing pad.*

In the analysis of Figure 7 it was observed that the largest change in $L_{\mathrm{eq},A}$ is likely due to greater low-frequency content as the aircraft passes over the microphone. It is of interest to show the OTO levels before and after the jet passes over the microphone to investigate possible changes in the spectrum. Figure 10 shows the spectra for the two peaks seen before (t = -40 s) and after (t = -32 s) the jet flyover in Figure 4(c) for the microphone at 250 ft and 30° and for the time of the lowest level at (t = -37 s). Though some differences are seen in the spectra, these are due to interference nulls due to path length differences. These interference nulls change frequency with the location of the aircraft relative to the microphone and are likely the cause of spectral differences, rather than a fundamental change in the noise. Interestingly, the spectrum at $t = -37$s, which represents the level minimum as the aircraft passes over, does not have the distinct characteristic frequency associated with jet noise.

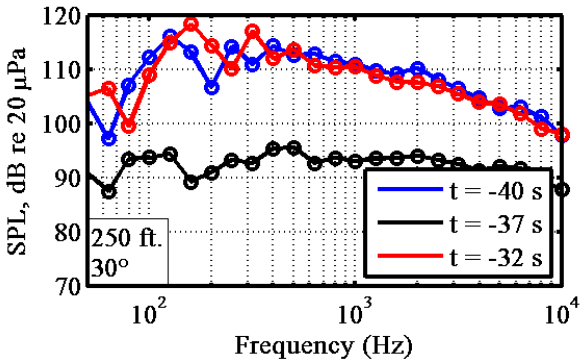

Figure 10. Comparison of sound pressure levels as aircraft passes over a microphone. *The 1.0s one-third octave spectra of the microphone at 250 ft and 30°, plotted before and after the flyover at the times indicated. The increase in low-frequency content explains the larger difference between flat and A-weight levels shown in Figure 7.*

Another important spectral feature seen at all microphones is the presence of low-frequency noise as the aircraft descends (see Figure 8 and Figure 9). This additional low-frequency noise corresponds to the spike in L_{eq} seen in Figure 4 and Figure 5 at $t\sim$ -8 s as the aircraft descends, which was previously attributed to impingement of the jet plume on the landing surface. Figure 11 shows a comparison of the spectrum of the microphone at 500 ft and 90° between two points in time. The first at $t = -25$s shows the spectrum as the aircraft begins its descent, and the second at $t = -8$s at the point where the spike in L_{eq} is seen in Figure 5(b). The spectral shape associated with the spike in L_{eq} is fundamentally different than that seen at the beginning of the descent. In particular, though much of the noise seems at a similar or slightly lower level, peaks are seen at approximately 125 and 250 Hz at much higher levels than at the beginning of the descent. This observation indicates a fundamental change in the noise source, but the peaks observed are not as discrete as those typically associated with impingement noise[10] and are at a lower frequency than might be expected. While phenomena associated with impingement could still be responsible for the change in source characteristics, a more thorough understanding of these processes is necessary for STOVL aircraft.

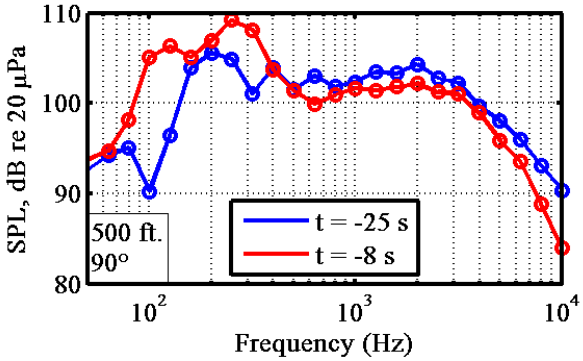

Figure 11. Sound pressure level variation during descent. *One-third-octave 1.0s SPL of the microphone at 500 ft and 90° is plotted for two different times. The first time at $t = -25$s is the beginning of the aircraft descent, and the second at $t = -8$s is shown towards the end of the descent, when a large spike in OASPL is seen in Figure 5. The low-frequency bands at $t = -8$s show an increase over the first, possibly caused by impingement of the jet plume on the landing pad.*

C. Azimuthal Directivity Modeling

An important aspect in modeling noise from a military jet are the variations in the noise azimuthally around the aircraft. Though in many measurements of military aircraft the variation with polar angle is of interest, in the case of vertical landings the plume is directed towards the ground, and the angle measured in the horizontal plane is now the azimuthal angle. The following plots examine the directivity of noise for the hover and the descent segments of the VL operation, which is unique to the F-35B and the AV-8B aircraft. The L_{eq} shown are normalized to a propagation distance of 250 ft for a standard acoustic day. All normalized L_{eq} are then plotted against the aircraft's azimuthal angle (0° is the nose of the aircraft), which is used to describe the sound field near an aircraft[16,17].

The overall sound pressure level is plotted against azimuthal angle for the Hover condition in Figure 12. Data from VLs 1, 2, and 4 are shown. VL3 had no clearly defined Hover segment duration so its data are not included. A large scatter is observed in the normalized data because of variations in the polar angles among the three arcs. However, a linear fit for all of the data within two standard deviations (σ) of the mean shows slight directivity trend with noise level increasing as the azimuthal angle increases.

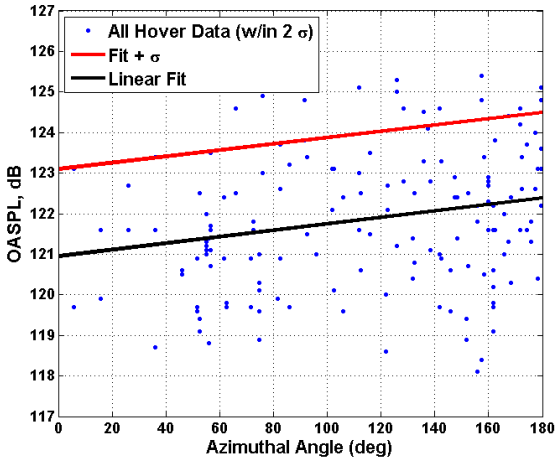

Figure 12. Directivity of the F-35B during hover. *The OASPL for all microphones during the hover process is corrected to 250 ft on a standard acoustic day, assuming spherical propagation and estimating absorption using weather data measured at the time of the test. All data within two σ are plotted against the NoiseFile angle, measured in the horizontal plane with* 0° *indicating in front of the nose of the aircraft. A linear fit of the data shows a slight increase in directivity behind the aircraft. This fit plus σ, the recommended levels for modeling the data, is plotted as a red line.*

During the descent process little directivity is observed. Data shown in Figure 13 are taken from all four VLs, but because airplane heading during the descent is dependent on wind direction, no data were obtained for the front of the aircraft. Using the data available, a linear fit produces no change from 0° to 180°, indicating no directivity in the azimuthal direction can be discerned.

For initial environmental noise modeling for the hover and descent, it is recommended that the source noise for these conditions utilize the linear fit with a positive offset of one standard deviation, which are obtained from the normalized data pool for each condition. These recommendation arises from the large scatter observed in the data and to provide a margin of safety for environmental analyses. These recommended modeling source levels are indicated by the red lines in Fig. 11 and 12.

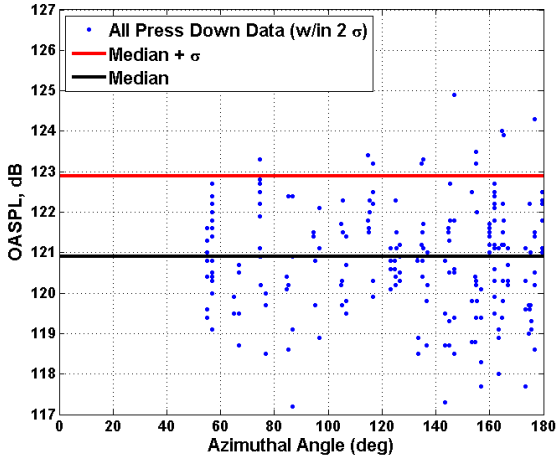

Figure 13. Directivity during the descent process. *The OASPL of each microphone is corrected as in Figure 12, but for the descent process. These data are plotted against NoiseFile angle, and a linear fit shows little directivity. Again, the recommended levels for modeling are the fit plus σ.*

D. Nonlinearity

The waveform steepening caused by nonlinear propagation has been investigated as the source of "crackle", an annoying auditory component of full-scale jet noise.[18,19] Many of these investigations have sought to identify shock waves using statistical metrics,[14,20] such as the average steepening factor[21] (ASF) and the skewness of the first time-derivative of the waveform,[22] referred to derivative skewness (dSk). Calculations of ASF and dSk during the VL provide insights into the prominence of nonlinearity. Similar to the level and spectral-based analyses presented above, ASF and dSk values are calculated using quarter-second intervals. To represent the strength of the observed shocks, both metrics are shown in Figure 14 and Figure 15 for two of the microphones located under the trajectory of the aircraft.

The dSk and ASF values seen at the 1000 ft, microphone, along the 30° arc, are significant. In all four runs, both metrics indicate the presence of steepened waveforms near the time that the plane passes overhead. However, at later times the values for both the dSk and ASF fall back into the noise floor. Small increases are seen in both dSk and ASF after the descent process begins, but the values seen are minimal, indicating that for these microphones, the steepest waveforms occur shortly prior to the aircraft passing overhead. From the presence of the second peak in the L_{eq} after the plane passes [at t = -47 s in Figure 4(a)], the absence of a second peak in the dSk and ASF is initially surprising as the spectra in Figure 8(a) exhibit similar-high frequency content associated with both peaks. However, given the downward orientation of the nozzle, it is possible that residual turbulence along the propagation path caused by the exhaust plume is strong enough to disrupt the coherent nonlinear waveform steepening process.

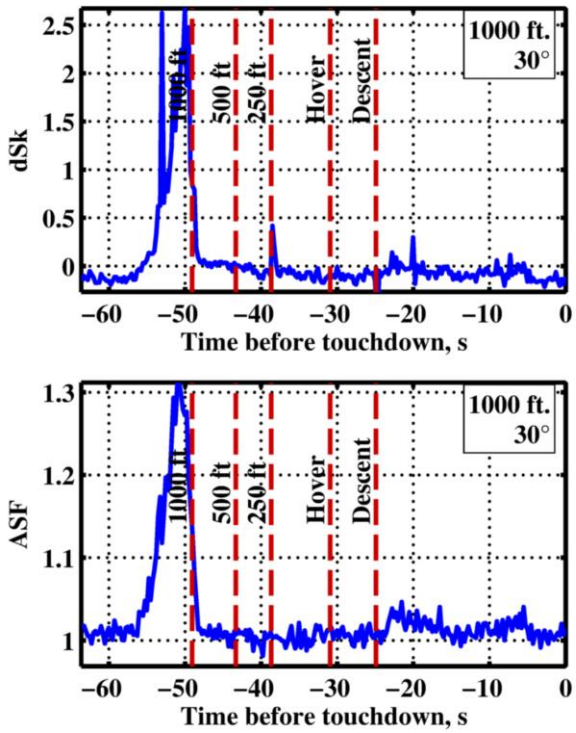

Figure 14. Nonlinearity metrics at 1000 ft. *The values of dSk and ASF are calculated using quarter-second intervals and plotted against time for a microphone located 1000 ft away from the landing pad. Large spikes in both metrics can be seen as the aircraft approaches the microphone, indicating steepened waveforms. However, both indicators show only minor increases during the descent process.*

The data from the microphone at 250 ft, along the 30° arc, show a similar spike shortly before the aircraft passes overhead but also contain information about the nonlinearity as the aircraft completes the descent process. Nonnegligible values of both dSk and ASF are seen at this microphone as the aircraft lands. As the aircraft lands the polar angle at which the microphone is located relative to the jet exhaust centerline axis changes with time. The polar angle of the microphone in the 250 ft arc ranges from roughly 51° to almost 90°. As the polar angle changes, the directivity of the aircraft noise causes a change in level, which results in the variation in the derivative skewness. The range of dSk values seen as the aircraft passes over the microphone are roughly consistent with the values reported by Gee *et al.* for the F-35 AA-1, measured at ~125 ft for an ETR of 50%.[14] The range of values for the ASF are between those calculated for 25% and 50% ETR.

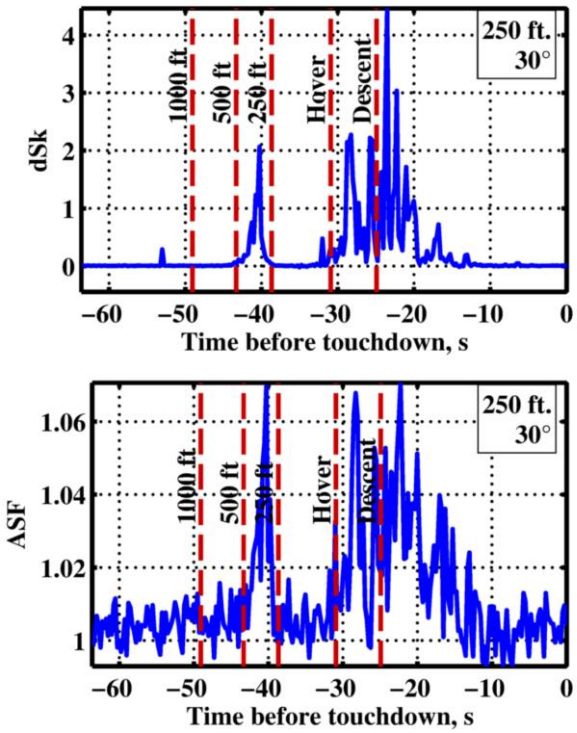

Figure 15. Nonlinear metrics at 250 ft. *Values are calculated in the same way as Figure 14 for the microphone located at 250 ft along the* 30° *radial.. A spike is again observed in both metrics as the aircraft approaches the microphone, but the descent process also produces higher values at this microphone, indicating the presence of steepened waveforms during the event.*

During the descent process, both nonlinearity metrics show significant values for the microphone located at 250 ft, corresponding to an engine condition operating between 25% and 50% ETR. Due to a combination of greater distance and greater polar angle, the nonlinearity metrics of the microphone at 1000 ft show only minimally steepened waveforms, leading to the conclusion that for the descent process, nonlinear effects are more important closer to the aircraft.

IV. Conclusions

This paper presents the first pressure measurements made near an F-35B during the process of a vertical landing. As the aircraft passes over microphones, L_{eq} values observed agree with levels observed around an F-35 AA-1 during at approximately 50% ETR, consistent with the published thrust conditions from an F-35B during a VL. Two peaks in L_{eq} are seen shortly before and after the aircraft passes over the microphone, with a reduction in level shortly after the jet passes over associated with the cone of silence near the jet plume. As the aircraft begins its descent, little azimuthal directivity is seen in the microphones. An increase in the L_{eq} seen shortly before touchdown at all microphones indicates plume impingement on the landing pad as the aircraft elevation reaches approximately 50 ft. A change in spectral content confirms the changing nature of the noise source, but the discrete tones normally associated with impingement are absent. Shortly after the increase in L_{eq} becomes noticeable but before the aircraft lands, a dramatic reduction in level is seen across all microphones, likely due to destruction of the turbulent noise source as the aircraft elevation continues to decrease. Values seen for nonlinear metrics both as the aircraft passes over microphones and during its descent again agree with values measured near an F-35 AA-1 running near 50% ETR, further validating comparisons made using the L_{eq} between the inflight and ground run-up data. These analyses may be used in assessing noise levels for ground personnel as well as the near-landing acoustical environments.

Acknowledgments

The authors would like to gratefully acknowledge funding for the measurements, provided through the F-35 Program Office and Air Force Research Labs. (Distribution A - Approved for Public Release; Distribution is Unlimited; JSF14-506.) B.O. Reichman was funded through by an appointment to the Student Research Participation Program at the U.S. Air Force Research Laboratory, 711th Human Performance Wing, Human Effectiveness Directorate, Warfighter Interface Division, Battlespace Acoustics Branch administered by the Oak Ridge Institute for Science and Education through an interagency agreement between the U.S. Department of Energy and USAFRL. The assistance of the NAVAIR Noise Team during measurements is also gratefully acknowledged.

References

[1] Gee, K. L., Sparrow, V. W.,James, M. M., Downing, J. M., Hobbs, C. M., Gabrielson, T. B., and Atchley, A. A.,"Measurement and prediction of noise propagation from a high-power jet aircraft," AIAA Journal, Vol. 45, No. 12, 2007, pp. 3003-3006.

[2] Gee, K. L., Sparrow, V. W., James, M. M., Downing, J. M., Hobbs, C. M., Gabrielson, T. B., and Atchley, A. A., "The Role of Nonlinear Effects in the Propagation of Noise from High-Power Jet Aircraft," Journal of the Acoustical Society of America, Vol. 123, No. 6, 2008, pp. 4082-4093.

[3] McKinley, R., McKinley, R., Gee, K. L., Pilon, T., Mobley, F., Gillespie, M., and Downing, J. M., "Measurement of Near-field and Far-field Noise from Full Scale High Performance Jet Engines," Proceedings of ASME Turbo Expo 2010. June 2010, Paper No. GT2010-22531.

[4] Wall, A.T., Gee, K.L., James, M.M., Bradley, K.A., McInerny, S.A., and Neilsen, T.B., "Near-field noise measurements of a high-performance military jet aircraft," *Noise Control Engineering Journal*, Vol. 60, No. 4, 2012, pp. 421-434

[5] Schlinker, R. H., Liljenberg, S. A., Polak, D. R., Post, K. A., Chipman, C. T., and Stern, A. M., "Supersonic Jet Noise Source Characteristics & Propagation: Engine and Model Scale," AIAA Paper 2007-3623, May 2007.

[6] "Proven Power for the F-35 Lightning II – In Flight, In Production," https://www.pw.utc.com/Content/Press_Kits/pdf/me_f135_pCard.pdf [cited 3 April 2015]

[7] "Rolls-Royce LiftSystem Technology", http://www.rolls-royce.com/customers/defence-aerospace/products/combat-jets/rolls-royce-liftsystem/technology.aspx

[8] Henderson, B, "An experimental investigation into the sound producing characteristics of supersonic impinging jets," AIAA 2001-2145, May 2001

[9] Marsh, A., "Noise measurements around a subsonic air jet impinging on a plane, rigid surface," Journal of the Acoustical Society of America, Vol. 33, 1961, pp. 1065-1066.

[10] Henderson, B., "The connection between sound production and jet structure of the supersonic impinging jet," Journal of the Acoustical Society of America, Vol. 111, No. 2, 2002, pp. 735-747

[11] Krothapalli, A., Rajkuperan, E., Alvi, F., and Lourenco, L., "Flow field and noise characteristics of a supersonic impinging jet," Journal of Fluid Mechanics, Vol. 392, 1999, pp. 155-181.

[12] Henderson, B., Bridges, J., Wernet, M., "An experimental study of the oscillatory flow structure of tone-producing supersonic impinging jets," Journal of Fluid Mechanics, Vol. 542, 2005, pp. 115-137

[13] Picture retrieved from http://www.navy.mil/view_image.asp?id=157440 [cited 3 April 2015]

[14] Gee, K.L., Neilsen, T.B., Reichman, B.O., Muhlestein, M.B., Thomas, D.C., Downing, J.M., James, M.M., and McKinley, R.L., "Comparison of Two Time-domain Measures of Nonlinearity in Near-field Propagation of High-power Jet Noise," AIAA Paper 2014-3199

[15] James, M.M., Salton, A.R., Downing, J.M., Gee, K.L., Neilsen, T.B., Reichman, B.O., McKinley, R.L., Wall, A.T., and Gallagher, H.L, "Acoustic Emissions from F-35A and F-35B during ground run-up," Proceedings of the 21st AIAA/CEAS Aeroacoustics Conference, (Submitted for publication 2015)

[16] Lundberg, W.R., Drye, D., "Verification of Noise Forecast Capabilities for Application to Full-scale Supersonic-capable Jet Engine Development," AIAA/3AF Aircraft Noise and Emissions Reduction Symposium, June

[17] Air Force Research Laboratory, NOISEFILE Database, Wright-Patterson AFB, OH, (2003).

[18] Ffowcs-Williams, J. E., J. Simson and V. J. Virchis, "'Crackle': An annoying component of jet noise," Journal of Fluid Mechanics, Vol. 71, No. 2., 1975, pp. 251-271.

[19] Gee, K. L., Neilsen, T. B., Muhlestein, M. B., Wall, A. T., Downing, J. M., James, M. M., and McKinley, R. L., "On the Evolution of Crackle in Jet Noise from High-Performance Engines," AIAA Paper 2013-2190, May 2013.

[20] McInerny, S. A., Gee, K. L. Dowing, J. M., and James, M. M., "Acoustical nonlinearities in aircraft flyover data," AIAA Paper 2007-3654, May 2007.

[21] Muhlestein, M.B., Gee, K.L., Neilsen, T.B., Thomas, D.C., "Evolution of the average steepening factor for nonlinearly propagating waves," Journal of the Acoustical Society of America, Vol. 137, No. 2 , 2015, pp. 640–650.

[22] Reichman, B. O., Muhlestein, M. B., Gee, K. L., Neilsen, T. B., and Thomas, D. C., "Evolution of the pressure derivative skewness for nonlinearly propagating waves," submitted to Journal of Acoustical Society of America (2014).